Ring closure of rolled-up Si/Cr nanoribbons

Li Zhang,[a] Lixin Dong,[b] and Bradley J. Nelson[c]
Institute of Robotics and Intelligent Systems, ETH Zurich, CH-8092 Zurich, Switzerland

(Received 12 March 2008; accepted 18 March 2008; published online 10 April 2008)

Nanobelts formed by the ring closure of rolled-up Si/Cr nanoribbons are fabricated on a Si (001) substrate. Interlayer bonding strengths are investigated by tangential unrolling and radial stretching using nanorobotic manipulation. Experimental results confirm that the multiwalled Si/Cr nanobelts can be considered physically closed structures and have strong interlayer bonding. The load versus deformation curve of nanobelts of varying ribbon widths reveals that the radial stiffness fulfills Hooke's law for small deformations. The measured radial stiffness of the nanobelts is also comparable to that of ideal seamless rings. © *2008 American Institute of Physics*.
[DOI: 10.1063/1.2906906]

Ringlike micro-/nanostructures synthesized or self-assembled from various materials have stimulated extensive investigation.[1,2] Techniques based on self-scrolling thin films have recently been developed to fabricate freestanding three-dimensional (3D) micro-/nanostructures, which have potential applications in micro-/nanoelectromechanical systems (MEMS/NEMS).[3,4] Edge effects have been discovered for Si-based ribbonlike patterns with ribbon widths in submicron to nanometer ranges, leading to the formation of 3D nanostructures such as small pitch coils[5] and spirals.[6] Using these edge effects, ring-closed rolled-up nanoribbon structures, i.e., nanobelts, can also be fabricated from a nanoribbon in any orientation on a Si (001) substrate. Although previous work[7] has shown that ringlike structures could be fabricated from a strained SiGe nanoribbon aligned to ⟨110⟩, no investigations have been performed on ring-closed structures due to this anomalous coiling. From a geometrical point of view, a multiwalled nanobelt can be regarded as a spiral nanoribbon with no gap between adjacent turns. In developing these types of structures, it is important to probe the interaction between the rolled-up layers and the radial stiffness. In this paper, the mechanical properties of individual as-fabricated Si/Cr multiwalled nanobelts are characterized using nanorobotic manipulation. Tangential unrolling and radial stretching are used to investigate their structure closure and interlayer bonding strength. An ideal ring structure model is used for comparison with the tightly scrolled structure.

The fabrication of multiwalled Si/Cr nanobelts is based on the coiling up of a Si/Cr nanoribbon of uniform ribbon width [Fig. 1(a)]. Details on the fabrication procedure have been described elsewhere.[5,6] Figure 1(b) presents a scanning electron microscope (SEM) image of a Si/Cr nanobelt with a ribbon width of 400 nm (w=400 nm) and approximately 2.5 turns. The SEM micrograph of this nanobelt clearly resolves that each turn of the nanobelt is tightly overlapped. A nanorobotic manipulator (Kleindiek MM3A) installed inside a SEM is used for mechanical property characterization of the nanobelt. A sharp tungsten probe is held by the manipulator and can be positioned with three degrees of freedom at nanometer resolution. Initially, to characterize the flexibility and the interaction of the neighboring layers of as-fabricated Si/Cr nanobelts, a tungsten probe mounted on the manipulator is inserted into the nanobelt, as shown in Fig. 2(a). Then, the probe is translated along the longitudinal axis of the nanoribbon to unroll the structure. It can be seen that the multiwalled (2.5 turn) Si/Cr nanobelt is highly deformed during the unrolling process. The maximum relative elongation of the nanobelt along this direction is approximately 75%, as shown in Fig. 2(d). When the nanobelt is extended to less than one circumference, its curvature elastically recovers to its original shape, as can be seen in Fig. 2(e). The unrolling tests reveal that the adjacent bilayers of the Si/Cr multiwalled nanobelt are bonded together, forming a closed ring structure. The adhesion force is relatively strong, particularly for nanobelts with ribbon widths in the micrometer range. For example, a Si/Cr nanobelt with a ribbon width of 1.1 μm, as shown at bottom-left corner in Fig. 2(a), was fractured at its fixed end before it could be unrolled. The result implies that van der Waals forces are not the sole contribution to the adhesion of adjacent bilayers, because both the van der Waals force and the tensile rigidity of the nanoribbon linearly increase with the increasing ribbon width. We attribute another possible interaction between the bilayers to hydrogen bonding because the rolled-up objects were formed after a wet etching and drying process. It is presumed that water molecules remain and link to one another to form a bridge between the adjacent bilayers[8] due to the imperfect surface roughness of the thermally evaporated Cr layer. The condensed liquid significantly increases the contact area, resulting in a large increase in adhesion.[8] When the width of the Si/Cr nanoribbon is larger than a critical value, the interaction bonding force will overwhelm the fracture force of the nanoribbon under tension. Thus, it is reasonable to assume that for multiple-turn Si/Cr or SiGe/Si/Cr micro-/nanotubes, the bonding force between the neighboring turns is sufficient to maintain closure before fracture, although the

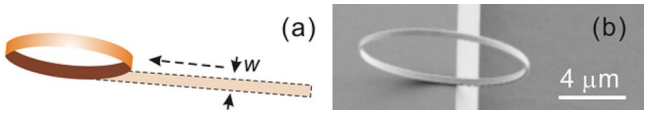

FIG. 1. (Color online) (a) Schematic drawing of the formation of a nanobelt rolled up from a nanoribbon. The dashed arrow represents the scrolling direction of the ribbon. (b) FESEM image of a freestanding Si/Cr (35/10 nm) nanobelt with a ribbon width (w) of 400 nm.

[a]Tel. No.: +41 44 6323669. Electronic mail: lizhang@ethz.ch.
[b]Tel. No.: +41 44 6322539. Electronic mail: ldong@ethz.ch.
[c]Author to whom correspondence should be addressed. Tel. No.: +41 44 6325529. Electronic mail: bnelson@ethz.ch.

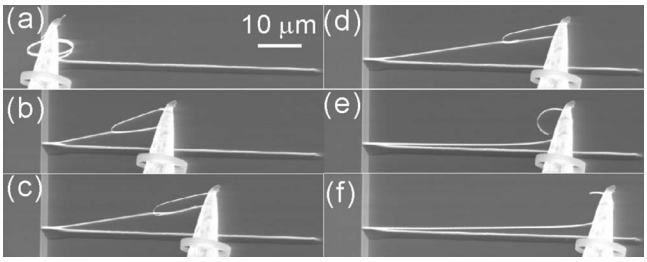

FIG. 2. SEM images showing the manipulator probe translating from left to right to unroll the Si/Cr nanobelt (w=500 nm). The white arrow in (a) points to another nanobelt with a ribbon width of 1.1 μm.

bonding force will be much smaller than covalent bonding in adjacent bilayers of the semiconductor micro/nanotubes.[9] Moreover, it is expected that the bonding energy at the interface of adjacent Si/Cr bilayer can be improved by thermal annealing, a process often used for wafer bonding.[8] The above manipulation results indicate that it is possible to use these micro-/nanotubes as pipelines[10] for microfluidic devices or as needles for microinjection.

To characterize the radial stiffness of a Si/Cr nanobelt under tensile load, an upright Si/Cr nanobelt with an indicating bar at the free end of the nanoribbon was prepared using a "T" shaped patterned bilayer. The nanoribbon is aligned 2.5° from ⟨110⟩. The mask design is shown in the inset of Fig. 3(a). This nanobelt has a diameter of 12.5 μm with a ribbon width of 1.2 μm. This design allows sliding between adjacent bilayers to be monitored by the movement of the crossbar when the structure is under tensile load. To perform the stretching test of the nanobelt, the nanobelt is cut and picked up with a "sticky" probe prepared by dipping the tip of the probe into a double-sided SEM silver conductive tape. The sticky probe is carefully attached to the outer sidewall of the nanobelt, and the probe is then moved along the scrolling direction of the nanoribbon to break the nanobelt from the substrate, as shown in Fig. 3(a). Unlike the unrolling test, the nanobelt is cut at its fixed end by applying a shear force with the nanomanipulator. Afterwards, the manipulator is used to bring the nanobelt to the backside of an atomic force microscope (AFM) cantilever so that the manipulator probe is on top of the nanobelt, and the AFM cantilever is at the bottom of the nanobelt [see Fig. 3(b)]. The other contact point of the nanobelt to the AFM cantilever is soldered by electron-beam induced deposition.[11] Then, the stretching test for the nanobelt is performed by moving the probe upward away from the AFM cantilever. The tensile load can be measured by the deflection of the AFM cantilever and its calibrated spring constant (0.038 N/m). The elongation of the nanobelt is measured along the loading direction.

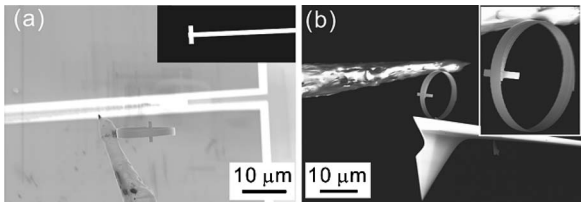

FIG. 3. (a) A Si/Cr nanobelt is cut from the substrate by a sticky probe. (Inset) The initial pattern design used to fabricate a Si/Cr nanobelt with a crossbar. (b) A Si/Cr ring is manipulated to the backside of an AFM cantilever with a manipulator probe. (Inset) Magnified image of the nanobelt with crossbar.

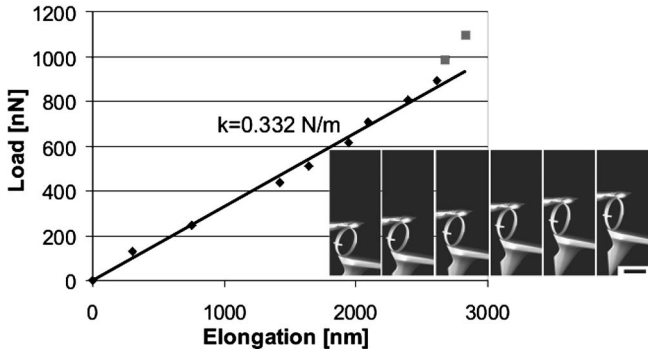

FIG. 4. Radial stiffness test of an individual Si/Cr nanobelt (35/10 nm). (Inset) A series of FESEM images with increasing tensile load on the Si/Cr nanobelt. The scale bar is 10 μm for all images.

A series of field emissin SEM (FESEM) micrographs in the inset of Fig. 4 shows the evolution of the process of subjecting a 2.5 turn Si/Cr nanobelt to an increasing tensile force. According to the manipulation tests, neither permanent deformation of the nanobelt nor clear sliding between the adjacent bilayers is observed, indicating that the multiwalled nanobelt remains closed during deformation under the applied load. It is expected that more energy is required to open a multiwalled nanobelt by a stretching test than an unrolling test, because the bonding energy must be simultaneously overcome between the adjacent bilayers. The radial stiffness of the 2.5 turn Si/Cr nanobelt is obtained by measuring the slope of the tensile load versus the corresponding elongation along the load direction, as shown in Fig. 4, revealing a linear relation when the relative elongation of the nanobelt is smaller than 23%. Thus, a corresponding radial stiffness of 0.332 N/m is determined using Hooke's law. However, the radial stiffness rapidly increases for deformations beyond 23%. The load versus elongation curve demonstrates that a Si/Cr nanobelt can perform as a mechanical spring when subjected to an external tensile load. When compared with a helical nanospring,[12] the nanobelt offers tunable stiffness by varying the number of the turns, wall thickness, and the ribbon width with only a small change in overall size. The increasing radial stiffness mainly results from the change of the force component from bending to tension in the region near points a and c [see Fig. 5(b)]. When the nanobelt experiences large deformations, the bending force gradually becomes tensile, and the curvature significantly changes, e.g., at point a and c in Fig. 5(b). Timoshenko analyzed an ideal seamless ring structure under small deformation from a compressive load P, where the radial stiffness k_r along the compression direction can be expressed as[13]

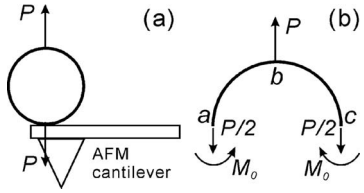

FIG. 5. (a) Schematic drawing of a ring undergoing a stretching test. (b) The upper-half ring structure is deformed due to the bending moment induced by the tensile load. The bending moments at point a and point c of the ring are the same, i.e., M_0.

$$k_r = (4EI)/[R^3(1-\nu^2)(\pi - 8/\pi)], \quad (1)$$

in which E is the Young's modulus, I is the moment of inertia of the cross sectional area of the ring, R is the radius of the ring, and ν is the Poisson ratio. If the ring has a rectangle cross section area with w ribbon width and h wall thickness, I is $wh^3/12$. For an ideal ring, the radial stiffness should be the same when applying compression or tension; thus, this equation is also valid as the nanobelt undergoes tensile deformation [see Figs. 5(a) and 5(b)]. The tensile stiffness of two straight belts connected in parallel with length (L) equal to πR (half circumference of the ring) is given by $k_t = 2EA/L = 2Ewh/\pi R$. The ratio of tensile stiffness to radial stiffness for this configuration is expressed as

$$\frac{k_t}{k_r} = \frac{2Ewh/\pi R}{Ewh^3/3R^3(1-\nu^2)(\pi - 8/\pi)} \approx 1.14(1-\nu^2)\left(\frac{R}{h}\right)^2. \quad (2)$$

For experimental analysis, the radius of the nanobelt and wall thickness is 6.25 μm and 45 nm/turn (35 nm Si and 10 nm Cr), respectively. It is known that the Poisson ratios of Si and Cr are less than 0.4; thus, the ratio of k_t to k_r is much larger than 1, i.e., $k_t \gg k_r$, indicating increasing radial stiffness for large deformations of the nanobelt. Considering the as-fabricated Si/Cr nanobelt as an ideal closed system, Eq. (1) is used to compare the experimental results. For a Si/Cr bilayer nanoribbon, Young's modulus of the Si layer along 2.5° from the ⟨110⟩ orientation is 168 GPa,[14] and a thermally evaporated Cr thin film has Young's modulus of 140 GPa. The Poisson ratios of the Si and the Cr layer are 0.06 (along ⟨110⟩) and 0.21, respectively. To simplify the calculation, we assumed that the Cr thin film has the same Young's modulus and Poisson ratio as the Si thin film, and the cross sectional area of the rolled-up nanobelt is considered to be a rectangle. Since the Si/Cr bilayer has a total thickness of 45 nm, a two-turn and a three-turn nanobelt have 90 and 135 nm total wall thicknesses, respectively. Calculations show that the radial stiffness of two-turn and three-turn Si/Cr nanobelt are 0.34 and 1.15 N/m, respectively. For the 2.5-turn rolled-up nanobelt, its radial stiffness in its linear region is very similar to a two-turn ideal ring. Since the bottom half of the nanobelt has one turn less than the upper half, the bottom half of the nanobelt is more compliant and undergoes the most deformation. Nevertheless, the upper half of the ring with larger wall thickness still deforms and increases the radial stiffness of the ring. Thus, the as-fabricated Si/Cr nanobelt as a whole is less stiff than the estimate. The overestimation of the radial stiffness is mainly attributed to the following factors: (1) In the calculation, Young's modulus of the Cr thin film increased from 140 to 168 GPa. (2) The flexural rigidity (EI) is proportional to the cubic power of the wall thickness of the nanobelt, and the real wall thickness may be slightly thinner than the calculated one due to the surface roughness of the Cr layer or due to the imperfect wet etching selectivity of the Si layer.[6] For example, for a wall thickness of 44 nm that is 1 nm thinner than the assumed value, the radial stiffness will be 6% less than the calculated result. In addition, a native amorphous chromium oxidation layer of 1–2 nm thick may form on the Si/Cr nanoribbon,[15] which may account for deviations of the estimated value from experimental results.

In conclusion, nanorobotic manipulation has been employed to characterize the mechanical properties of multiwalled Si/Cr nanobelts. Results show that the as-fabricated Si/Cr nanobelts exhibit excellent elasticity. Adjacent bilayers of the multiwalled Si/Cr nanobelt are strongly bonded, and bonding between adjacent bilayers does not break under tensile loads in the experiments. Manipulation tests of the 2.5 turn nanobelt also show that the ring-closed rolled-up nanoribbon performs as a mechanical spring, and its radial stiffness remains constant under small deformations. The excellent mechanical properties of these ring-closed nanostructures, the possibility of using different materials, and excellent compatibility with Si technology suggest that they are promising for MEMS/NEMS devices.

Some experiments were done at the Paul Scherrer Institute. The authors thank Dr. J. Gobrecht and Dr. D. Grützmacher for their support. They also thank E. Deckardt and A. Weber for their technical help.

[1] M. Sano, A. Kamino, J. Okamura, and S. Shinkai, Science **293**, 1299 (2001).
[2] X. Y. Kong, Y. Ding, R. Yang, and Z. L. Wang, Science **303**, 1348 (2004).
[3] V. Y. Prinz, V. A. Seleznev, A. K. Gutakovsky, A. V. Chehovskiy, V. V. Preobrazhenskii, M. A. Putyato, and T. A. Gavrilova, Physica E (Amsterdam) **6**, 828 (2000).
[4] O. G. Schmidt and K. Eberl, Nature (London) **410**, 168 (2001).
[5] L. Zhang, E. Ruh, D. Grutzmacher, L. X. Dong, D. J. Bell, B. J. Nelson, and C. Schonenberger, Nano Lett. **6**, 1311 (2006).
[6] L. Zhang, L. X. Dong, D. J. Bell, B. J. Nelson, C. Schoenenberger, and D. Gruetzmacher, Microelectron. Eng. **83**, 1237 (2006).
[7] O. G. Schmidt, C. Deneke, Y. M. Manz, and C. Muller, Physica E (Amsterdam) **13**, 969 (2002).
[8] Q. Y. Tong and U. Goesele, *Semiconductor Wafer Bonding* (Wiley, New York, 1999), p. 22.
[9] N. Y. Jin-Phillipp, J. Thomas, M. Kelsch, C. Deneke, R. Songmuang, and O. G. Schmidt, Appl. Phys. Lett. **88**, 033113 (2006).
[10] O. G. Schmidt and N. Y. Jin-Phillipp, Appl. Phys. Lett. **78**, 3310 (2001).
[11] L. X. Dong, F. Arai, and T. Fukuda, IEEE/ASME Trans. Mechatron. **9**, 350 (2004).
[12] D. J. Bell, L. X. Dong, B. J. Nelson, M. Golling, L. Zhang, and D. Grutzmacher, Nano Lett. **6**, 725 (2006).
[13] S. P. Timoshenko, *Theory of Elastic Stability*, 2nd ed. (McGraw-Hill, Kogakusha, Tokyo, 1961), p. 278.
[14] J. J. Wortman and R. A. Evans, J. Appl. Phys. **36**, 153 (1965).
[15] C. Deneke, W. Sigle, U. Eigenthaler, P. A. van Aken, G. Schutz, and O. G. Schmidt, Appl. Phys. Lett. **90**, 263107 (2007).